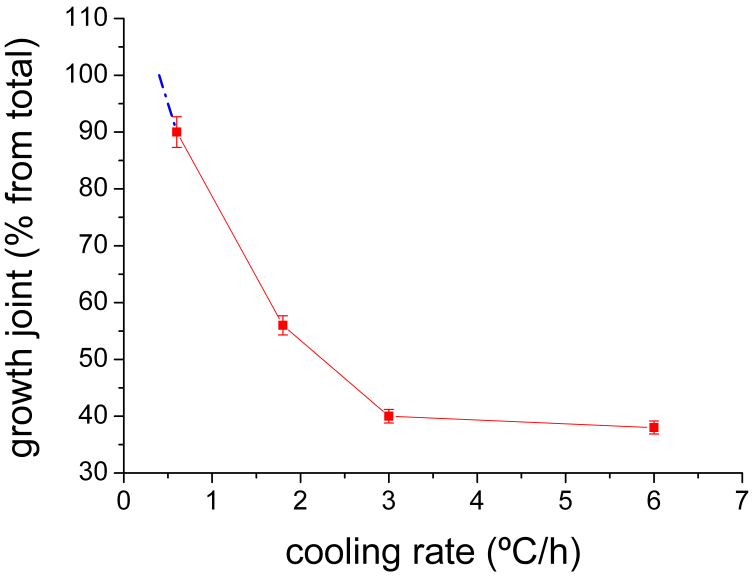

Figure 6.27: The influence of the cooling rate on the high quality joint dimensions.

particle size and interfacial energies between solid and liquid phases are crucial in this theory, which describes trapping or pushing of an inclusion by an advancing solid front through a liquid. It is based on the existence of a critical particle radius (d_c), i.e. the minimum particle radius required to be captured by the solid, the critical particle radius can be written as:

$$d_c \approx \frac{\Delta\sigma a_0}{3\eta R} \tag{6.5}$$

where $\Delta\sigma$=σ_{PS}-σ_{PL}-σ_{SL}, and σ_{PS}, σ_{PL}, σ_{SL}, are the particle/solid, particle/liquid and solid/liquid interface free energies, respectively. a_0 is the average intermolecular distance, η is the liquid viscosity, and R is the solidification growth rate. Equation 6.5 indicates that if the particle is larger than d_c ($d > d_c$), it is trapped by the growing front. Instead, if the radius of the particle is smaller than d_c ($d < d_c$), the particle remains indefinitely pushed by the interface.

Two antagonist forces acting on the particle are considered: a repulsive force due to the surface tension effects, F_{surf}=2πr$\Delta\sigma(\frac{a_0}{d})^n$, where d is the distance

between the particle and the solid/liquid interface and n is a free parameter close to 1. The second force is an attractive viscous drag force, F_{visc}= $\frac{6\pi\eta Rr^2}{d}$ arising from the fresh liquid flowing between the particle and the advancing front. Then, equation 6.5 is obtained by equating both forces at the critical condition a_0=d [52]. This theory was first applied to YBCO/211 composites by Endo et al [85] to study the anisotropic pushing of 211 particles and lately by Delamare *et al.* and Kim *et al.* [86, 87] also in relation to the 211 precipitates in MTG YBCO composites. Moreover, Nakamura et al [46] have applied this theory to study the Ag inclusions in MTG YBCO crystals.

According to equation 6.5, the pushing effect of Ag precipitates should be enhanced by decreasing the particle size below the critical radius, or increasing the critical radius by decreasing the cooling rate or melt viscosity. The best solution for this experiment, taking into account that the starting materials MTG YBCO are provided by "Nexans Superconductors" and IPHT Jena, with a standard composition described in Chapter 4, was to increase the critical radius by decreasing the cooling rate. The elimination of CeO_2 additives to reduce the melt viscosity, η, would generate some Y211 particle coarsening at the interface which can affect the supercurrent flow [87]. Additionally, the results obtained by Carrillo et al [88] showed that the growth rate has a stronger influence on the pushing efficiency than the modification of the melt viscosity in the YBCO material by reducing the CeO_2 initial amount.

The phenomenon of Ag liquid expulsion from the molten interface has been investigated in our laboratory by employing an in-situ video camera system allowing to observe the melting process at high temperature and to follow the metallic Ag distribution [73]. It was amazing to observe that the Ag rich liquid migrates from the interface due to capillarity forces and become distributed through the solid sample surface and the ceramic support. Moreover, by optical micrograph we have observed that the Ag liquid migrates through micro and macrocracks existing in the initial YBCO sample (see figure 6.9).

Indeed, according to our experiments, it has been demonstrated that by decreasing the cooling rate down to 0.6°C/h the resulting joints clearly displayed the highest growth quality encountered so far. Additionally, however, as it can be seen in figure 6.28, by reducing the cooling rate, the liquid loss increases at low cooling rates. This is obvious taking into account that the lower the cooling rate, the longer the time spent by the interface in the liquid state. It was interesting to observe that when the cooling rate is of 0.6°C/h the liquid lost by the sample was about 4% from the total weight of the sample. This means that all the Ag used as welding agent, which represents 2% from the total weight of the joint, is expelled from the sample during the processing schedule. Additionally, there is about another 2% of weight loss, which might be BaCuO_2-CuO liquid phase which could be pushed away together with liquid Ag. In any case, this represents a small amount of liquid loss. Accordingly, these liquid losses did not lead to any important degradation of the final microstructure of the joint. This demonstrates that the time that the interface has spent in the liquid state is long enough to push complete the Ag liquid, but short enough to avoid an excessive additional liquid loss which could result in a perturbed composition at the joint.

Electron microprobe analysis at the YBCO/Ag/YBCO interfaces obtained by using a cooling rate r=0.6°C/h agree with this conclusion. In figure 6.29 quantitative analysis of the YBCO/Ag/YBCO interface while crossing the weld are shown. The origin represents the point where the junction is situated. According to these results, the quantity of Ag found in the sample is lower than 0.008%at which represents ≈50% from the theoretical value of detection limit of the microprobe which is 0.016%at. Additionally, the value of the detection limit is below the solubility of Ag into YBCO (1-2%at) which means that a small amount of Ag could be detected by this technique if Ag migrates into YBCO matrix. For instance, the sample $C_{0.6}$ is free of any Ag precipitates which were pushed away during the welding process. The detection limit of the probe is calculated according to equation 3.1 as it was explained in Chapter 3. The difference in the

quantity of Ag found at the interface, as can be seen in figure 6.29, is not significant since all the values are below the detection limit of the probe.

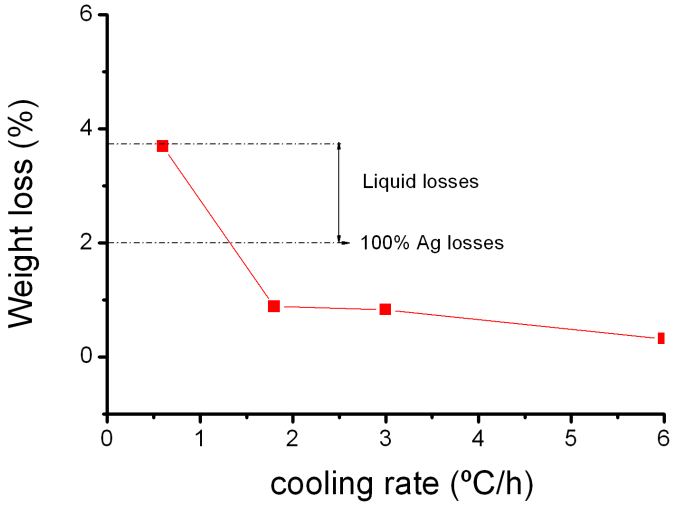

Figure 6.28: Liquid losses dependence with the cooling rate. If the sample losses more than 2% from its weight it will correspond to the lost of all the Ag used for joining.

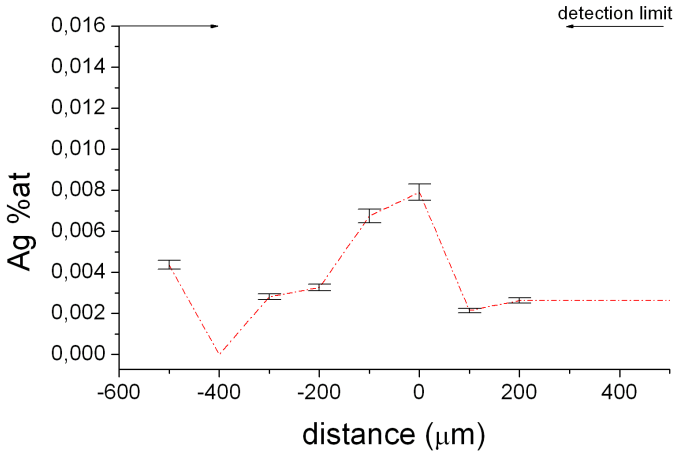

Figure 6.29: Electron microprobe analysis obtained for a joint cooled down at 0.6°C/h.

The surfaces corresponding to ac planes have been polished also in order to

observe the microstructure of the junction. For a better visualization of the small optically contrasted bands (hereafter called oxygenation bands), which are usually generated around regions having microcraks parallel to the ab planes which then facilitate a faster oxygenation [89], we have studied the microstructure before the oxygenation process. Moreover, the study has been carried out using optical microscopy with polarized light. These bands were described perviously by our group [40] and were used to observe the orientation of both YBCO single domains submitted to the welding process [68].

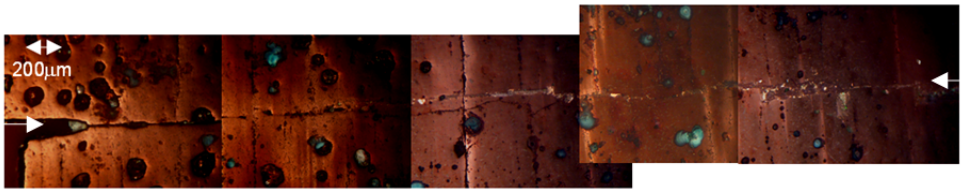

(a)

(b)

(c)

Figure 6.30: Optical micrographs corresponding to the (a,c) planes of joints obtained at different cooling rates: a) 6°C/h; b) 3°C/h; c) 0.6°C/h

Figures (6.30) illustrate the whole joining zone of the samples C_6 (6.30a), C_3 (6.30b) and $C_{0.6}$ (6.30c) respectively, obtained at different cooling rates. Regard-

ing the oxygenation bands, it can be observed in all the samples that they extend parallel at each side of the interface, sometimes crossing it. The observation of a tendency of these bands at the joined interface witnesses the dissimilar origin of both ceramic tiles. Also its parallelism indicates that the ab planes have the same orientation at both sides of the interface. As a consequence, the welding process did not deteriorate the YBCO solid, even if the applied process was not the optimum one.

A detailed study of the sample C_6 shows that there is no connectivity between YBCO grains as can be observed in figure 6.30a. Thus, the size of high quality joint is negligible. Observations at higher magnification of the interface are presented in figure 6.31. At the junction it is easy to observe the existence of bright zones, corresponding to non-superconducting phases formed during the welding process. These phases are characteristic of an unoptimized weld and correspond to Ag precipitates and $BaCuO_2 - CuO$ phases. Hence, we conclude that the time spent by the interface in the liquid state was too short to push completely the Ag liquid during the welding process.

By reducing the cooling rate to 3°C/h, the microstructure of the ac plane improves. The high quality joint size represents ≈64% from the total length of the joint. In figure 6.30b note that at the center of the junction the microstructure seems to be free of secondary phases. A higher magnification of the center (optical micrograph) and lateral parts (BSE micrograph) of the YBCO/Ag/YBCO interface corresponding to the sample C_3 is shown in figure 6.32. Note that at the center of the sample (figure 6.32a), the so-called oxygenation bands sometimes are continuous through the joint and sometimes do not cross the junction but are parallel, indicating that the ab planes have the same orientation at both sides of the interface. Moreover, no non-superconducting phases have been observed at the central part of the junction. On the contrary, some dark regions can be observed at edge of the interface and are extended up to 360 μm into the YBCO solid matrix (see figure 6.32b). WDS analysis of these regions have been

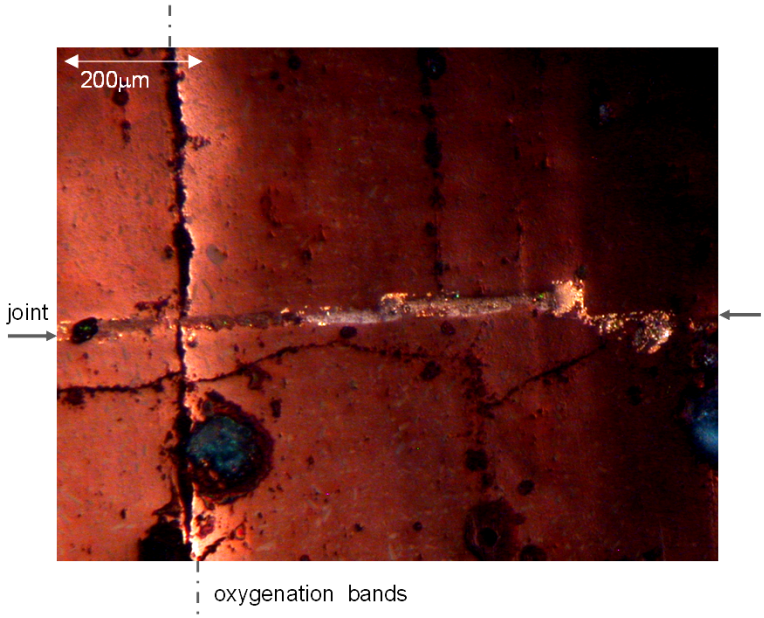

Figure 6.31: Optical micrograph of the ac plane of the sample C_6 showing the microstructure of the joining zone with more detail. The joint and the oxygenation bands are indicated in the figure.

performed (see figure 6.33) and show that there is a strong presence of Ag precipitates and $BaCuO_2$-CuO phases at the interface. Figure 6.33a shows the Ag map where the bright particles are Ag precipitates and figure 6.33b represents the Cu map where bright particles are associated with Cu. Thus, the Ag liquid was pushed from the center of the sample towards the edge of the interface and this part of the joint did not have time to crystallize because the cooling rate was too high and the time spent by the interface in liquid state was actually shorter than that required to push away all the Ag.

When studying the ac plane of the sample $C_{0.6}$ obtained at a cooling rate of 0.6°C/h, it was amazing to observe that it was free of any non-superconducting phase all along the interface. This means that the interface has crystallized all along its length and all the Ag has been pushed away from the interface. Furthermore, note in figure 6.34 that the oxygenation bands are parallel at each side of the joint indicating a perfect matching between YBCO monoliths submitted to

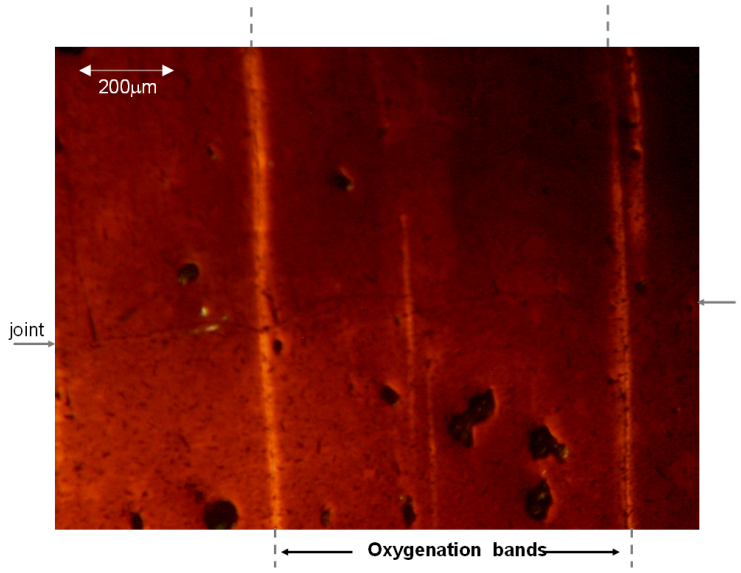

(a)

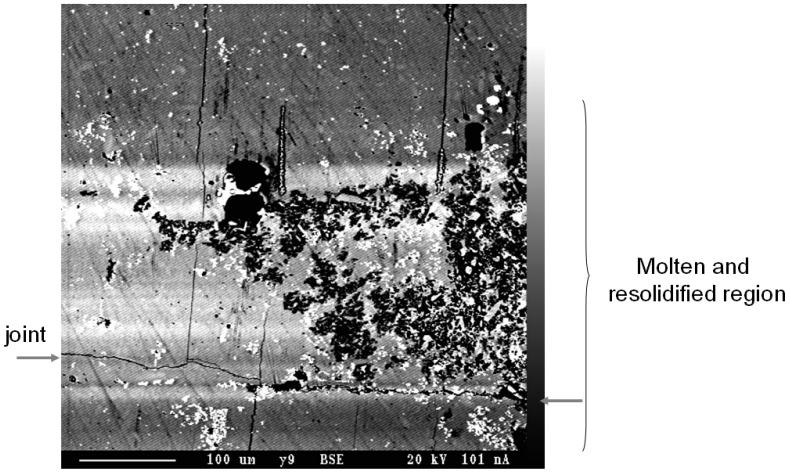

(b)

Figure 6.32: a) Optical micrograph of the ac plane of the sample C_3 showing the microstructure of the joining zone with more detail. The joint is indicated by arrows and the oxygenation bands are indicated also in the figure; b) BSE micrograph at the edge of the sample C_3 showing the presence of Ag and $BaCuO_2$-CuO phase which was pushed away by the growth interface. The joint and the molten and resolidified region are indicated in the figure.

the welding process.

Thus, for a given cooling temperature window of 33°C, the joints grown at dif-

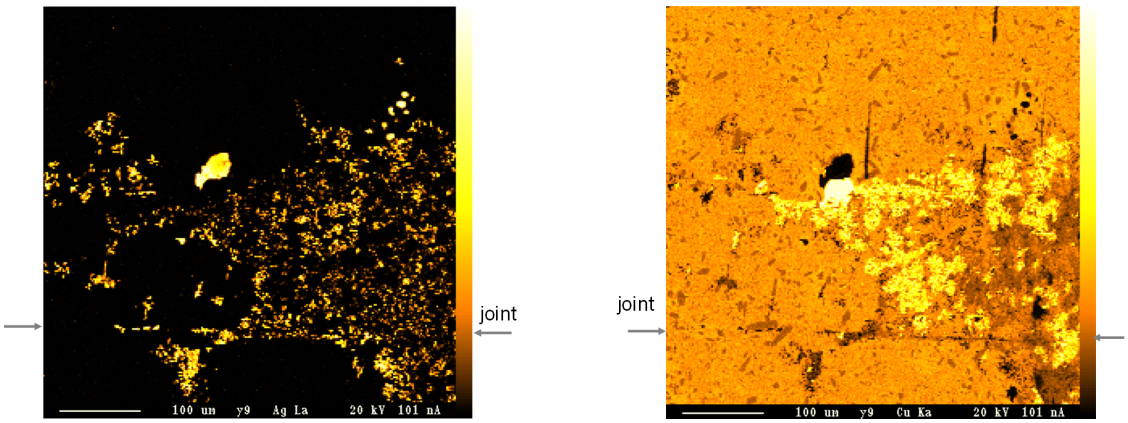

Figure 6.33: The map of elements of a YBCO/Ag/YBCO interface of the sample C_3: a) Ag precipitates; b) Cu precipitates.

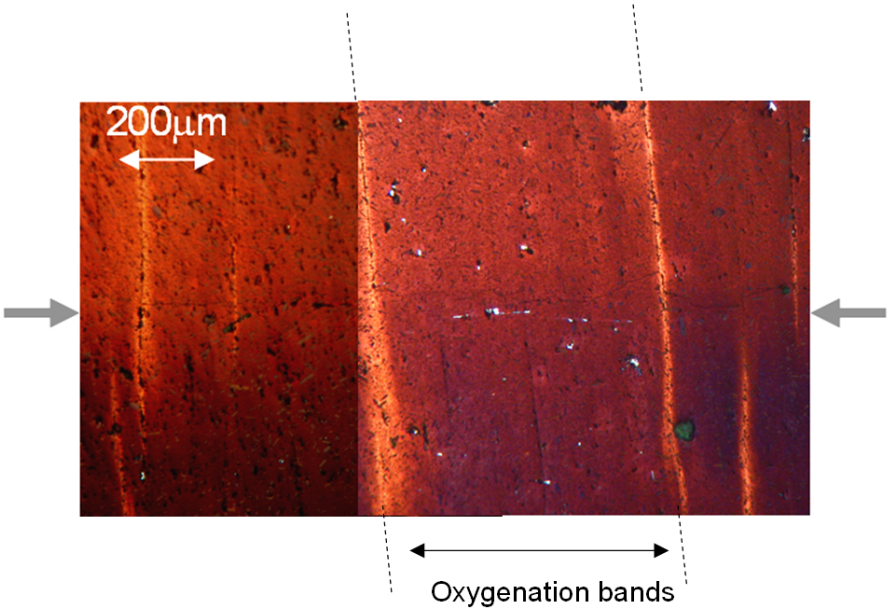

Figure 6.34: Optical micrograph showing the microstructure of the ac plane of the joint $C_{0.6}$ cooled down at 0.6°C/h. The joint is indicated by arrows and the dashed line indicates the oxygenation bands which are perpendicular to the junction.

ferent cooling rates appear to have different microstructures. The samples grown at higher cooling rates, have a reduced size of matched weld. As viewed from the microstructure analysis, it is considered that the cooling rate of 0.6°C/h is the

optimum one.

The samples grown at a sufficient low cooling rates showed in the central part of the junction regions free of Ag and $BaCuO_2$-CuO phases, in both ab and ac planes. When the cooling rate was of r=0.6°C/h, the junction was silver-free all along its length. The existence of silver-free region means that Ag rich liquid (L1 in the equation 6.4) was not captured into the YBCO crystal growth during the welding process. The probable mechanisms thought to form the Ag free regions on the junction [4] is based on the pushing trapping phenomenon studied by Ulhmann *et al.* [51]. Thus, the complete pushing of all L1 droplets dispersed in the L2 liquid ($BaCuO_2$-CuO) liquid phase as denoted in equation 6.4 towards the edges of the junction by the growing YBCO interfaces takes place during the welding process.

According to this phenomenon, is required that the L1 phase does not wet YBCO crystal when it is included in the L2 liquid. The YBCO crystal, therefore, pushes the L1 droplets with smaller size than the critical size which is determined by the UCJ type pushing mechanism [4], even though the L1 and L2 coexist in the front of the YBCO growing interface. This image is schematically drawn in figure 6.35 where the dark grey areas represent the YBCO matrix and the light grey areas represent the Ag and $BaCuO_2 - CuO$ phases which were pushed by the growth interface towards the edge of the sample. The distance x in the figure represents the welding crystallized area. If initially the existing L1 droplets are too small to be captured into the YBCO crystal, there would be no silver particles at the interface; i.e the silver free regions would be formed (distance x in the figure). During the growth of YBCO, the Ag-rich liquid pushed by the growing interface can grow in size by coalescing each other. When the size of L1 droplets reaches the critical one, they will begin to be trapped at the interface.

All L1 droplets initially existed in the L2 liquid must have smaller size than the critical one for pushing them outside the sample. Supposing that the T_{max} of

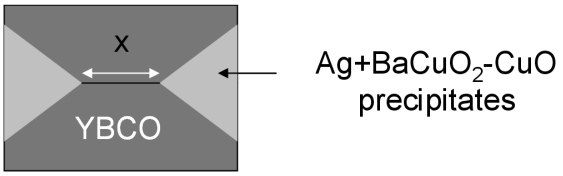

Figure 6.35: Schematic view of the pushing effect observed during the welding process. The dark grey areas represent the YBCO matrix whereas the light grey areas represent the Ag+$BaCuO_2 - CuO$ precipitates which were pushed by the growth front towards the edges of the sample.

the welding process and that the time spent by the interface in the liquid state are sufficiently high to reduce the size of the Ag droplets below the critical one, the phenomenon will be as follows: when the cooling rate starts, the junction is still in the liquid state. If Ag droplets exist in the L2 liquid, they will become large as cooling down the sample due to the enhanced concentration of Ag in the L2 liquid and pushing of L1 droplets. Moreover, at lower temperatures the viscosity of Ag is large. As a consequence we have to push away all the Ag from the interface before the droplets grow in size. If the cooling rate is too high, the dragging force on Ag liquid will be too high and then Ag-rich liquid is trapped at the interface. For instance, we should use a lower cooling rate in order to give time to the YBCO crystal growth to expel all the Ag from the interface.

Another mechanism thought to form Ag free-region is the complete dissolution of Ag in the L2 liquid at the maximum temperature. This mechanism has been proposed by Nakamura *et al.* [4] when YBCO/Ag single domains grown by using a TSMG process have been studied. Indeed, Ag dissolution is strong at high temperatures but according to quench experiments performed in this thesis was shown that Ag dissolution in our case was not complete since Ag precipitates have been found by EDX analysis (see figure 6.3).

As a consequence, the mechanism thought to form Ag free interfaces is the pushing-trapping phenomenon along with a partial Ag dissolution in L2 liquid at the maximum temperature.